

Quintessential Kination and Leptogenesis

Eung Jin Chun^{1,2} and Stefano Scopel¹

¹Korea Institute for Advanced Study
207-43 Cheongryangri-dong Dongdaemun-gu
Seoul 130-722, Korea

²Michigan Center for Theoretical Physics
Department of Physics, University of Michigan
Ann Arbor, MI 48109, USA

Abstract

Thermal leptogenesis induced by the CP-violating decay of a right-handed neutrino (RHN) is discussed in the background of quintessential kination, i.e., in a cosmological model where the energy density of the early Universe is assumed to be dominated by the kinetic term of a quintessence field during some epoch of its evolution. This assumption may lead to very different observational consequences compared to the case of a standard cosmology where the energy density of the Universe is dominated by radiation. We show that, depending on the choice of the temperature T_r above which kination dominates over radiation, any situation between the strong and the super-weak wash-out regime are equally viable for leptogenesis, even with the RHN Yukawa coupling fixed to provide the observed atmospheric neutrino mass scale ~ 0.05 eV. For $M \lesssim T_r \lesssim M/100$, i.e., when kination stops to dominate at a time which is not much later than when leptogenesis takes place, the efficiency of the process, defined as the ratio between the produced lepton asymmetry and the amount of CP violation in the RHN decay, can be larger than in the standard scenario of radiation domination. This possibility is limited to the case when the neutrino mass scale is larger than about 0.01 eV. The super-weak wash-out regime is obtained for $T_r \ll M/100$, and includes the case when T_r is close to the nucleosynthesis temperature ~ 1 MeV. Irrespective of T_r , we always find a sufficient window above the electroweak temperature $T \sim 100$ GeV for the sphaleron transition to thermalize, so that the lepton asymmetry can always be converted to the observed baryon asymmetry.

1 Introduction

Present observations strongly favour the existence of dark energy, which contributes a fraction $\Omega_{\text{DE}} \simeq 0.7$ to the closure density. This dark energy component in the present universe can be explained by modifying the standard cosmology with the introduction of a slowly evolving scalar field called quintessence [1]. This approach has been shown to have “tracking solutions” [2] that solve the so-called coincidence problem suffered by a pure cosmological constant, namely explaining in a natural way why radiation and dark energy provide comparable contributions to the energy budget of the present Universe, in spite of having very different time evolutions. An open possibility in this scenario is the existence of an early era of kination domination, during which the Universe is dominated by the kinetic energy of the quintessence field. During this era, the expansion rate of the Universe is larger compared to the usual radiation domination case. An interesting consequence of this fact is that the relic abundance of a Cold Dark Matter candidate can be significantly enhanced compared to the canonical prediction [3], because its decoupling time from the plasma is anticipated. In this way, for models with high detection rates, the relic density that is usually small in the standard case can be brought back to the range compatible to observation. This leads to interesting phenomenological implications for the LHC and other future collider or astrophysics experiments. Another interesting prediction of the kination domination scenario in inflationary models is the absence of a measurable tensor perturbation induced B-mode CMB polarization, which can be tested in the next-generation CMB experiments [4].

In this paper, we investigate the impact of the quintessential kination scenario on the properties of the thermal leptogenesis induced by the CP-violating decay of a right-handed neutrino (RHN), N [5]. In particular, when the RHN Yukawa coupling is fixed in order to explain the observed atmospheric neutrino mass scale $\simeq 0.05$ eV through the see-saw mechanism, leptogenesis is known to proceed in the strong wash-out regime for a standard Cosmology. As will be shown in the following, similarly to the case of the relic density of a thermal relic, the faster expansion rate in the early Universe due to kination dominance can modify the predictions for the standard leptogenesis scenario, even by several orders of magnitude. As a consequence of this, any situation between the strong and the super-weak wash-out regime are equally viable for leptogenesis in presence of kination domination.

The paper is organized as follows. In Section 2 the main features of the quintessential cosmological scenario are summarized, and the basic requirements for kination domination at early times are discussed. In Section 3 thermal leptogenesis is discussed in the context of an MSSM model supplemented by heavy right-handed neutrino supermultiplets with CP-violating decays, and the relevant Boltzmann equations are introduced. Section 4 is devoted to our discussion, where the solutions for the Boltzmann equations of leptogenesis for a kination dominated Universe are compared to those for the standard radiation dominated case. We summarize our conclusions in Section 5.

2 Kination and leptogenesis

Let us begin with a brief summary of the cosmological behavior of kination. The kination regime is attained when, in the energy-momentum tensor of the quintessence field ϕ (assumed here as spatially constant): $T_{\mu\nu} = \partial_\mu\phi\partial_\nu\phi - g_{\mu\nu}\mathcal{L}$, the kinetic term $\dot{\phi}^2/2$ dominates over the potential term $V(\phi)$, so that

$$w \equiv \frac{p}{\rho} = \frac{\frac{\dot{\phi}^2}{2} - V(\phi)}{\frac{\dot{\phi}^2}{2} + V(\phi)} \rightarrow 1. \quad (1)$$

Eq. (1) must be compared to the corresponding values for radiation ($w = 1/3$), vacuum ($w = -1$) and pressure-less dust ($w = 0$). The energy density of the Universe scales like $\rho \propto a^{-3(1+w)}$, which, in particular, implies

$$\begin{aligned} \rho_{rad} &\propto a^{-4} && \text{(radiation)} \\ \rho_{kin} &\propto a^{-6} && \text{(kination)}. \end{aligned} \quad (2)$$

In the following, we will assume that, in the epoch after reheating which is relevant to thermal leptogenesis, the energy density of the Universe is dominated by the sum of the above two components, $\rho = \rho_{rad} + \rho_{kin}$, with the boundary condition:

$$\rho_{kin}(T_r) = \rho_{rad}(T_r), \quad (3)$$

where the kination-radiation equality temperature T_r is in principle a free parameter, with the only constraint: $T_r \gtrsim 1$ MeV, in order not to spoil big-bang nucleosynthesis. Eqs. (2,3) imply

$$\rho(T) = \rho_{rad}(T) + \rho_{rad}(T_r) \left(\frac{a_r}{a}\right)^6, \quad (4)$$

where $\rho_{rad}(T) = \pi^2/30g_*T^4$. Assuming an isentropic expansion of the Universe, $(a^3s)=\text{constant}$, with $s = 2\pi^2/45g_*T^3$, we get

$$g_*a^3T^3 = g_{*r}a_r^3T_r^3 \rightarrow \left(\frac{a_r}{a}\right)^6 = \left(\frac{g_*}{g_{*r}}\right)^2 \left(\frac{T}{T_r}\right)^6, \quad (5)$$

where g_* is the number of relativistic degrees of freedom, while a_r and g_{*r} are the values of a and g_* at temperature T_r . Thus one finds the dependence of ρ on the temperature T as

$$\rho(T) = \frac{\pi^2}{30}g_*T^4 \left(1 + \frac{g_*}{g_{*r}} \left(\frac{T}{T_r}\right)^2\right). \quad (6)$$

The above form of the energy density drives the expansion of the Universe through the Hubble parameter given by

$$H(T) = 1.66\sqrt{g_*} \frac{T^2}{m_{pl}} \sqrt{1 + \frac{g_*}{g_{**}} \left(\frac{T}{T_r}\right)^2}, \quad (7)$$

where $m_{pl} = 1.22 \times 10^{19}$ GeV. By introducing the non-dimensional quantity $z \equiv M/T$, where M is the mass of the heavy neutrino producing leptogenesis, the scaling of H , which will be relevant to the solution of the Boltzmann equation discussed in the next section, can be expressed in the simple form:

$$H(z) = \sqrt{\frac{z^2 + z_r^2}{1 + z_r^2}} \frac{H_1}{z^3}, \quad (8)$$

where $H_1 \equiv H(z=1)$ and $z_r \equiv \sqrt{\frac{g_*}{g_{**}}} M/T_r$.

The main consequence of Eqs. (7,8) is that, whenever $T > T_r$, the expansion rate is dominated by kination, and can be much faster compared to radiation. In particular, taking $T_r = 1$ MeV, $g_{**} = 10.75$ and $g_*(T) = 228.75$ in the supersymmetric standard model, we get

$$H(T) \simeq 0.95 \times 10^4 \text{ GeV} \left(\frac{3.28 \text{ MeV}}{\sqrt{g_{**}} T_r}\right) \left(\frac{T}{10^6 \text{ GeV}}\right)^3. \quad (9)$$

This value must be compared to the rate of gauge interactions, that insure thermalization after reheating. Their scattering rate is approximately given by $\Gamma_{gauge} \approx \alpha^2 T$, so that the requirement $\Gamma_{gauge} > H$ leads to the following upper limit on the reheat temperature and thus on the RHN mass:

$$M \simeq T < 3.4 \times 10^5 \left(\frac{\sqrt{g_{**}} T_r}{3.28 \text{ MeV}}\right)^{1/2} \text{ GeV}, \quad (10)$$

for $\alpha = 1/30$. The bound of Eq. (10) implies that in the quintessential kination scenario thermal leptogenesis is viable for masses which are typically lower than in the standard case. Of course, the above constraint on M can be relaxed when $T_r \gg 1$ MeV, as the conventional picture of radiation domination is recovered for $z_r \rightarrow 0$. Moreover, in order to allow the conversion of the lepton asymmetry to the baryon asymmetry, the electroweak sphaleron interaction must be in thermal equilibrium before the electroweak phase transition. Taking the order of magnitude estimate of the sphaleron interaction rate $\Gamma_{sp} \sim \alpha^4 T$ [6], the condition $\Gamma_{sp} > H$ reduces the above constraint (10) by an additional factor α :

$$T < 10^4 \left(\frac{\sqrt{g_{**}} T_r}{3.28 \text{ MeV}}\right)^{1/2} \text{ GeV}. \quad (11)$$

Therefore, we get a sufficient window for the sphaleron transition to thermalize above the electroweak temperature $T \sim 100$ GeV even for $T_r = 1$ MeV.

3 Supersymmetric kination leptogenesis

In this paper we wish to discuss thermal leptogenesis in the Minimal Supersymmetric extension of the Standard Model (MSSM) supplemented by right-handed neutrino supermultiplets, i.e. the model described by the following superpotential:

$$\mathcal{W} = \mathcal{W}_{MSSM} + \frac{1}{2} N^c M N^c + y H_2 L N^c. \quad (12)$$

This scenario has been extensively studied in the literature [7, 8] in a conventional cosmological setup where the energy density of the early Universe is dominated by radiation. We wish now to discuss leptogenesis in the scenario of kination domination introduced in the previous section. Let us remark that our results can also be applicable to the non-supersymmetric case without any qualitative change.

In the MSSM, the decay rate of a RHN is given by $\Gamma_d = |y|^2 M/4\pi$ where y is the neutrino Yukawa coupling. Introducing as usual the effective neutrino mass scale given by

$$\tilde{m} \equiv |y|^2 \frac{\langle H_2 \rangle^2}{M}, \quad (13)$$

and using Eq. (8), we can get the ratio $K \equiv \Gamma_d/H(z=1)$:

$$K = \frac{63.78}{\sqrt{1+z_r^2}} \left(\frac{\tilde{m}}{0.05 \text{ eV}} \right). \quad (14)$$

We remind that the standard cosmology is recovered in the above equation when $z_r \ll 1$, and thus leptogenesis proceeds in the strong wash-out regime, $K \gg 1$, for \tilde{m} equal to the observed atmospheric neutrino mass scale. The situation changes for kination domination, where $z_r \gg 1$. In particular, putting numbers in the above equation one gets:

$$K = 1.38 \times 10^{-6} \left(\frac{10^4 \text{ GeV}}{M} \right) \left(\frac{\tilde{m}}{0.05 \text{ eV}} \right) \left(\frac{\sqrt{g_{*r}} T_r}{3.28 \text{ MeV}} \right). \quad (15)$$

Thus, if kination dominates the energy density of the Universe until nucleosynthesis, leptogenesis is in the super-weak wash-out regime, $K \ll \ll 1$, even when $\tilde{m} \simeq 0.05 \text{ eV}$. On the other hand, assuming $T_r \gg 1 \text{ MeV}$, higher values of K can be attained, so that a broad range of different scenarios are possible. However, as will be shown in the discussion of Section 4, an upper bound $K \lesssim 10$ exists if kination has to play any rôle for leptogenesis.

The Boltzmann equations that drive leptogenesis involve the comoving densities $Y_i(z = M/T) \equiv n_i/s(z)$, with n_i the density of the species i , s the entropy density, and $i=N$ (heavy Majorana neutrinos), \tilde{N} (sneutrinos), \tilde{N}^\dagger (anti-sneutrinos), l (leptons), \bar{l} (anti-leptons), \tilde{l} (sleptons) and \tilde{l}^\dagger (antisleptons). The additional degrees of freedom h_2, h_2^\dagger (Higgs bosons) and \tilde{h} (higgsino) need not to be studied, since their densities are constrained to be equal to $\tilde{l}, \tilde{l}^\dagger$ and l . All other light degrees of freedom are assumed in thermal equilibrium. It is convenient to introduce the following adimensional densities:

$$\begin{aligned} N(z) &\equiv \frac{Y_N(z)}{Y_N^{eq}(z=0)}, & \tilde{N}(z) &\equiv \frac{Y_{\tilde{N}}(z)}{Y_{\tilde{N}}^{eq}(z=0)}, & \tilde{N}^\dagger(z) &\equiv \frac{Y_{\tilde{N}^\dagger}(z)}{Y_{\tilde{N}^\dagger}^{eq}(z=0)}, \\ \tilde{N}_\pm &\equiv \tilde{N}(z) \pm \tilde{N}^\dagger(z), & L(z) &\equiv \frac{Y_l(z) - Y_{\bar{l}}(z)}{Y_l^{eq}(z=0)}, & \tilde{L}(z) &\equiv \frac{Y_{\tilde{l}}(z) - Y_{\tilde{l}^\dagger}(z)}{Y_{\tilde{l}}^{eq}(z=0)}. \end{aligned} \quad (16)$$

The Boltzmann equations of the system can be simplified by noticing that MSSM gaugino-mediated interactions of the type $l + l \rightarrow \tilde{l}\tilde{l}$ are very fast and can be safely assumed to be in thermal equilibrium. This automatically implies that $\tilde{N}_- = 0$ and $L = \tilde{L}$. Thus setting now

$$\begin{aligned} \hat{N}(z) &\equiv N(z) + \tilde{N}_+ \\ \hat{L}(z) &\equiv L(z) + \tilde{L}(z), \end{aligned} \quad (17)$$

the Boltzmann equations driving the system are given by

$$\frac{d\hat{N}}{dz}(z) = -K \sqrt{\frac{1+z_r^2}{z^2+z_r^2}} z^2 (\hat{N} - \hat{N}_{eq}) [\gamma_d(z) + 2\gamma_s(z) + 4\gamma_t(z)] \quad (18)$$

$$\frac{d\hat{L}}{dz}(z) = K \sqrt{\frac{1+z_r^2}{z^2+z_r^2}} z^2 \left[\gamma_d(z) \epsilon (\hat{N} - \hat{N}_{eq}) - \frac{\gamma_d(z) \hat{N}_{eq} \hat{L}}{4} - \frac{1}{2} \gamma_s(z) \hat{L} \hat{N} - \gamma_t(z) \hat{L} \hat{N}_{eq} \right]. \quad (19)$$

where the CP-violating parameter ϵ is defined as in Ref. [7], $\gamma_d(z) = K_1(z)/K_2(z)$ ($K_{1,2}$ are Bessel functions of the first kind) and $\hat{N}_{eq}(z) = z^2 K_2(z)/2$. Here, we have included the dominant lepton-number violating scattering amplitudes $\gamma_{s,t}$ proportional to the top Yukawa coupling λ_t and driven by Higgs exchange, which are

given by:

$$\gamma_{s,t}(z) \equiv \frac{1}{n_{eq}\Gamma_d} \frac{T}{64\pi^4} \int ds \hat{\sigma}_{s,t}(s) \sqrt{s} K_1\left(\frac{\sqrt{s}}{T}\right) \quad (20)$$

where $n_{eq}(z) = \frac{g}{2\pi^2} \frac{M^3}{z} K_2(z)$ with $g = 2$ (either Majorana ν or $\tilde{\nu} + \tilde{\nu}^\dagger$)

and $\hat{\sigma}_{s,t}(s) \equiv 3 \frac{\alpha_u}{4\pi} f_{s,t} \left(\frac{s}{M^2} \right)$, $\alpha_u = \frac{\lambda_t^2}{4\pi}$.

In the above equations the functions $f_{s,t}$ are given by:

$$f_s(x) \equiv 3 \left[f^{(0)}(x) + \frac{f^{(3)}(x)}{2} + f^{(5)}(x) + \frac{f^{(8)}(x)}{2} + \frac{f_{22}(x)}{2} \right]$$

$$f_t(x) \equiv \frac{3}{2} \left[f^{(1)}(x) + f^{(2)}(x) + f^{(4)}(x) + f^{(6)}(x) + f^{(7)}(x) + f^{(9)}(x) + f_{22}(x) \right]. \quad (21)$$

where the functions $f^{(i)}$ can be read-off from Eqs. (C.20-C.30) and Eq. (14) of Ref. [7]. In our calculation, we include the thermal effect by taking $a_h \equiv m_H(T)/M$ [8], where $m_H(T) \simeq 0.4 T$ is the thermal mass for the Higgs/Higgsino particles. We remark that in our analysis the difference between bosons and fermions is neglected, as we work in the Boltzmann approximation. The main effect of the quantity a_h is to regularize the infrared divergence in the t-channel, which shows up in the logarithms in the functions $f^{(i)}$. In particular, when a_h is neglected everywhere with the exception of the logarithms, the functions $f_{t,s}$ take the simplified form:

$$f_s \equiv 6 \frac{x-1}{x}$$

$$f_t \equiv 6 \left[-1 + \log \frac{x-1+a_h}{a_h} \right]. \quad (22)$$

However, in our numerical calculations, we kept a_h everywhere (although the above simplified form leads to very similar conclusions). Note that scattering effects may be safely included at the tree-level, and at this order of perturbation theory they are CP-conserving processes.

The effect of thermal corrections on the other masses, as well as on the CP-violating parameter ϵ , has been considered in the literature [8], and can be important, especially at high temperatures. However, in our case the bulk of leptogenesis takes place at temperatures low enough to suppress any sizable effect on the final result, so in the following we will neglect thermal effects, with the exception of the introduction of the coefficient $a_h(T)$. The functions γ_d and $f_{s,t}$ are plotted in Fig. 1 as a function of z . Fig. 1 shows that the effect of scattering is particularly important at higher temperatures, where the amplitudes $\gamma_{s,t}$ are larger than γ_d . On the other hand, at lower temperatures the effect of scattering turns out to be negligible.

4 Properties of leptogenesis: kination vs. radiation

In this section we discuss the solutions of the Boltzmann Eqs. (18,19) for some illustrative examples. We mainly concentrate here on the case of a vanishing initial RHN density, $\hat{N}(0) = 0$, and give some comments also for the case $N(0) = 1$ (initial thermal distribution for the RHN). Besides solving them numerically for the more general cases, it is useful to work-out semi-analytic solutions of Eqs. (18,19) in the limits $K \ll 1$ and $K \gg 1$ in the two cases of radiation domination ($z_r \ll 1$) and kination domination ($z_r \gg 1$).

(i) Super-weak wash-out regime.

In the case $K \ll 1$, leptogenesis takes place early, when $z \lesssim 1$ (see discussion of Figs. 2 and 3). As a consequence of this, in Eq.(18) one can neglect $\hat{N} \ll \hat{N}_{eq}$, so that it decouples from Eq.(19). Setting:

$$\Delta \equiv \hat{N} + \frac{\hat{L}}{\epsilon}, \quad (23)$$

one gets for the efficiency η the solution:

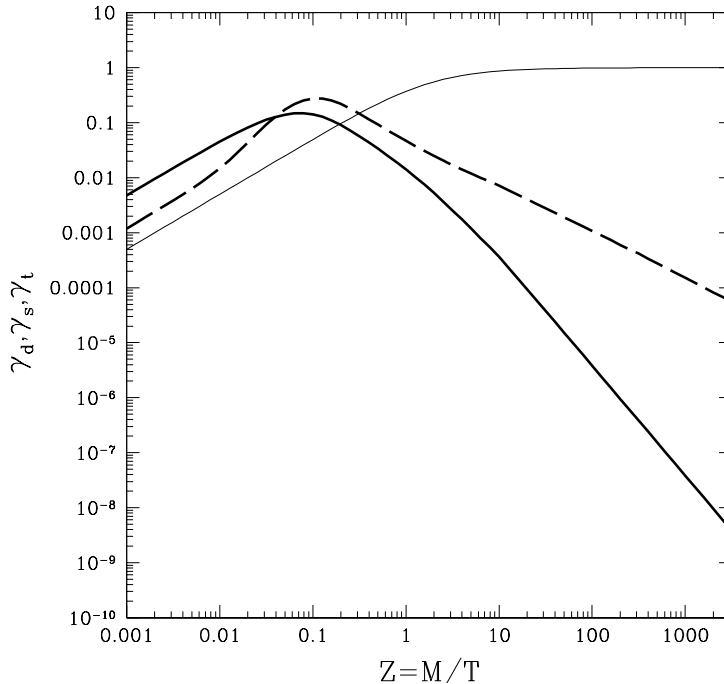


Figure 1: Decay and scattering rates γ_d (thin solid line), γ_s (thick solid line), γ_t (thick dashed lines) used in the Boltzmann equations (18,19), as a function of z .

$$\begin{aligned}
 \eta &\equiv \frac{\hat{L}(\infty)}{\epsilon} = \Delta(\infty) \simeq K \int_0^\infty z^n \hat{N}_{eq}(z) (\gamma_d + 2\gamma_s + 4\gamma_t) dz \simeq K \int_0^\infty z^{n+2} K_2(z) (\gamma_s + 2\gamma_t) \\
 &= K \hat{I}_n \quad \text{with} \quad \hat{I}_1 \simeq 0.504, \text{ and } \hat{I}_2 \simeq 0.921,
 \end{aligned} \tag{24}$$

where $n = 1$ and 2 for radiation and kination domination, respectively. In the second integral of Eq. (24) γ_d has been dropped, since the integral takes its main contribution at $z \lesssim 1$ where scattering amplitudes dominate. So, for $K \ll 1$, scattering turns out to be essential in determining the efficiency η . Eq. (24) is consistent with the result of Ref. [9], which in particular showed how η is proportional to K^2 or K , depending on whether scattering terms are neglected or included, respectively.

To see more in detail the behavior of the numerical solutions of Eqs. (18,19) in the two cases of kination- and radiation-domination, we show them for $K = 10^{-6}$ in Figs. 2 and 3. In particular, in the former the scattering effect is neglected, while in the latter it is included. In both figures the evolution of the different quantities \hat{N} , \hat{L}/ϵ and Δ is shown as a function of z , and the left hand panel shows the result obtained by assuming $z_r \ll 1$ ($n = 1$) in the Boltzmann equations (radiation domination), while the right hand panel is calculated for $z_r \gg 1$ ($n = 2$) (kination dominated).

Some general features, valid for both kination and radiation, can be realized by comparing these figures. In both cases, at higher temperatures an initial population of RHNs and an early lepton asymmetry are built up. This process is active as long as the initial light states have enough kinetic energy to create RHNs, i.e., as long as $z = M/T < 1$. By the time when $z \simeq 1$ and this process stops, RHNs have neither thermalized nor decayed due to their very weak couplings, so both the RHN density and the lepton asymmetry are frozen as can be seen from their evolution in Figs. 2 and 3 which show a plateau until much later ($z \gg 1$).

In Fig. 2 where the scattering processes are not included in the calculation, one can see that the asymmetry \hat{L}/ϵ tracks closely \hat{N} until the decay of RHNs. Moreover, when RHNs decay, they produce a lepton asymmetry that cancels the one created earlier due to inverse decays by several orders of magnitude. It is worth noticing here that inverse-decay rates are proportional to the densities of initial states, so the inverse-decay rate for

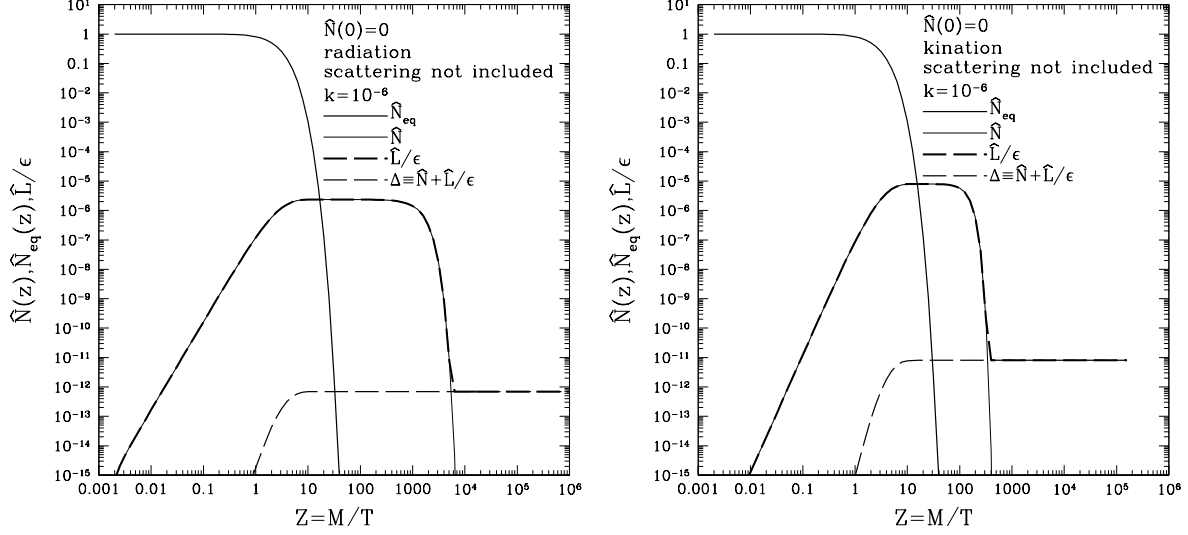


Figure 2: Evolution as a function of $z \equiv M/T$ of the quantities \hat{N} , \hat{L}/ϵ , $\Delta \equiv \hat{N} + \hat{L}/\epsilon$, for the case $K = 10^{-6}$, and neglecting scattering. Left panel: energy density dominated by the radiation field; right panel: energy density dominated by kination.

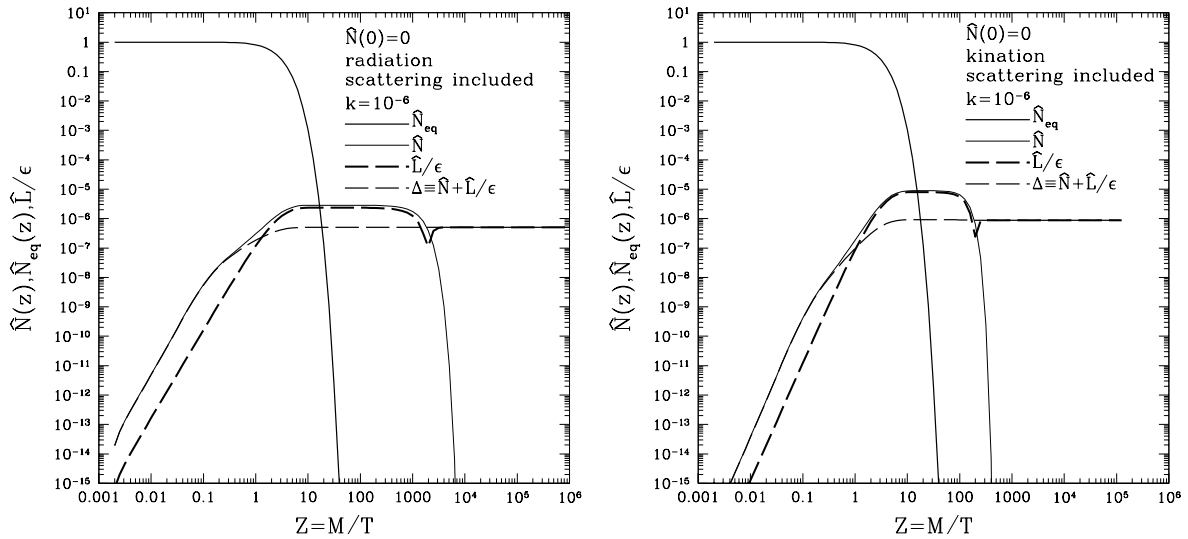


Figure 3: The same as in Fig. 2 with the inclusion of the scattering effect.

a particle whose reaction is faster than its anti-particle (due to CP violation) is suppressed by the higher depletion in the corresponding population. This implies that the effective amount of CP violation in the early inverse-decay processes is slightly smaller than ϵ . On the other hand, when the RHNs decay out-of-equilibrium at later times the amount of CP violation is exactly given by ϵ . So the lepton asymmetry created later has opposite sign and slightly overshoots the earlier one (actually, the wiggle that is visible in the evolution of \hat{L}/ϵ signals a sign change, since it is plotted in absolute value). It is this mismatch that explains why in this plot the asymmetry created at early times by inverse decays is not exactly canceled by RHN decays at later times. Anyway, the final value of the asymmetry is given by a very strong cancellation, and is essentially produced by a second-order back-reaction effect. In particular, it can be seen that, when scattering is neglected, $\hat{L}/\epsilon \propto K^2$ [9], which implies a strong suppression for $K \ll 1$.

The inclusion of scattering processes in the solution of the Boltzmann equations changes the property described above. First of all, due to the higher overall interaction rate, the RHNs are more populated in the first place, and this enhances the final asymmetry. However, the main effect which is active now is due to the presence of s -channel scatterings of the type $Q + U \rightarrow N + L$. In fact, this last type of interactions, which is dominant for $z \lesssim 0.2$ (see Fig. 1) is (approximately) a CP-conserving process. This means that it populates \hat{N} without affecting \hat{L}/ϵ (since, for instance, $\Gamma(Q + U \rightarrow N + L) = \Gamma(\bar{Q} + \bar{U} \rightarrow N + \bar{L})$). As a consequence of this, in both panels of Fig. 3 now the asymmetry \hat{L}/ϵ no longer tracks \hat{N} (this may be appreciated in Fig. 3 at early times, when $z \lesssim 0.2$, and s -channel scattering processes are dominant). When these RHNs decay at later times, they produce a lepton asymmetry that is not canceled by an earlier, specular one, left over by their earlier production. This explains why in Fig. 3 almost all the asymmetry produced for $z \lesssim 0.2$ survives until later times, while that created later is washed out. As a consequence of this, including scattering processes the efficiency is much higher and the characteristic drop in the asymmetry when RHNs decay is much less pronounced.

By comparing the two panels of Fig. 3, one can see the effect of different cosmological models on the evolution of the lepton asymmetry. The final values of the efficiency are quite similar in the two cases. As estimated in Eq. (24), the difference between kination and radiation in the final asymmetry is expected to be about a factor of 2 for fixed K . Moreover, the plateau in the evolution of the asymmetry corresponds to a shorter interval in z in the case of kination compared to radiation: this is due to the fact that, in the time interval given by the RHN lifetime, the Universe is decelerating faster for kination, implying less expansion and cooling, so that the corresponding variation of the z parameter is smaller.

(ii) Strong wash-out regime:

For $K \gg 1$, the semi-analytic solutions of the Boltzmann equations (18,19) can be calculated using the saddle point technique. In this case the bulk of the lepton asymmetry is produced at the decoupling temperature z_f , determined by the approximate relation:

$$z_f^{n+\frac{3}{2}} e^{-z_f} = \frac{2^{\frac{7}{2}}}{K\pi^{1/2}}, \quad (25)$$

(where again $n = 1$ for radiation and $n = 2$ for kination) which can be approximated by the logarithmic fits:

$$\begin{aligned} z_f &\simeq a_n + b_n \ln(K), \\ a_1 &= 1.46; \quad b_1 = 1.40, \\ a_2 &= 4.66; \quad b_2 = 1.41. \end{aligned} \quad (26)$$

By comparing Eqs. (14) and (26) it is possible to set an upper bound on K , as anticipated in the previous section. In fact, by fixing K in both equations and requiring that $z_f < z_r$ (i.e., that decoupling happens in the regime of kination domination), one gets the inequality:

$$z_f \simeq a_2 + b_2 \ln(K) < \sqrt{\left(\frac{63.78}{K} \frac{\tilde{m}}{0.05 \text{ eV}}\right)^2 - 1} = z_r. \quad (27)$$

This numerically implies, for instance, $K \lesssim 7.6$ for $\tilde{m} = 0.05$ eV, and $K \lesssim 5.7$ for $\tilde{m} = 0.01$ eV. The inequality (27) has no solution for $K > 1$ when $\tilde{m} \lesssim 0.004$ eV.

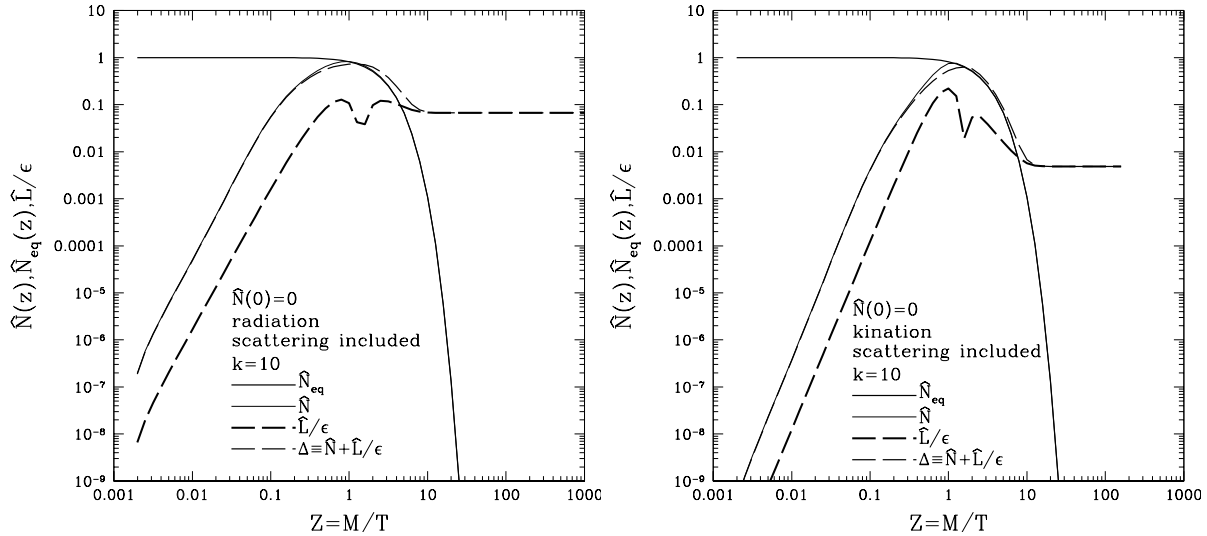


Figure 4: The same as in Fig. 3, for the case $K = 10$.

For $K \gg 1$, the final value of the efficiency is given by the approximate expression:

$$\eta = \frac{\hat{L}(\infty)}{\epsilon} = \hat{N}_{eq}(z_f) F_{wash-out}(n, z_f), \quad (28)$$

$$\text{where } \hat{N}_{eq}(z_f) = \frac{4}{K z_f^n}, \quad (29)$$

$$\text{and } F_{wash-out}(n, z_f) \simeq \sqrt{\frac{2\pi}{1 - \frac{n}{z_f}}} \exp \left[- \left(1 + \frac{\frac{3}{2} + n}{z_f} \right) \right]. \quad (30)$$

An example of the numerical solutions of Eqs. (18,19) in the strong wash-out regime is shown in Fig. 4 for $K = 10$, in the case of kination domination (left panel) and radiation domination (right panel). As opposed to Fig. 3, now RHNs quickly thermalize, and produce a lepton asymmetry when they decouple at $z \simeq z_f \gg 1$. In Fig. 4 the scattering effect is included, but does not affect the final asymmetry, since the latter may develop only at late times when the scattering processes are negligible.

By comparing the two panels one can see that, as implied by Eq. (26), RHNs stay in thermal equilibrium longer for kination than for radiation. This is explained by the fact that the two models have the same Hubble-expansion rate at $z = 1$ (when K is defined) but decoupling happens at $z > 1$, when the model dominated by kination is decelerating faster and has a slower expansion compared to the case of radiation domination. Moreover, the RHN equilibrium density for $z > 1$ is further suppressed for kination compared to radiation [see Eq. (29)]. This implies a sizeable difference in the final lepton asymmetry between kination and radiation, in contrast to what happens in the case $K \ll 1$ for which the difference is less pronounced. Note also that, since the RHNs thermalize at $z \simeq 1$, erasing any dependence of the final asymmetry on earlier boundary conditions, the calculated efficiency would be the same assuming $\hat{N}(0)=1$.

In order to summarize the temperature-dependence of the solutions of the Boltzmann equations (18,19), we present in Fig. 5 the evolution of Δ as a function of z for $K = 10^{-6}$ (solid line), 1 (long dashes), 10 (long dashes), in the case of radiation domination (thin lines) and kination domination (thick lines), and when the boundary condition $\hat{N}(0) = 0$ is adopted. The same plot for the case $\hat{N}(0) = 1$ is shown in Fig. 6. In the latter case, for $K \ll 1$ one has $\Delta=1$ during the whole range of z , and both for radiation and kination. This corresponds to the ideal case when the initial equilibrium density of RHNs decay out of equilibrium with efficiency 1. For $K \gtrsim 1$ and as long as the RHNs reach thermalization, the efficiency is the same as for the case with $\hat{N}(0) = 0$ already discussed. In particular, as already mentioned, in this case the efficiency for kination is lower compared to radiation because of the later decoupling for the RHNs.

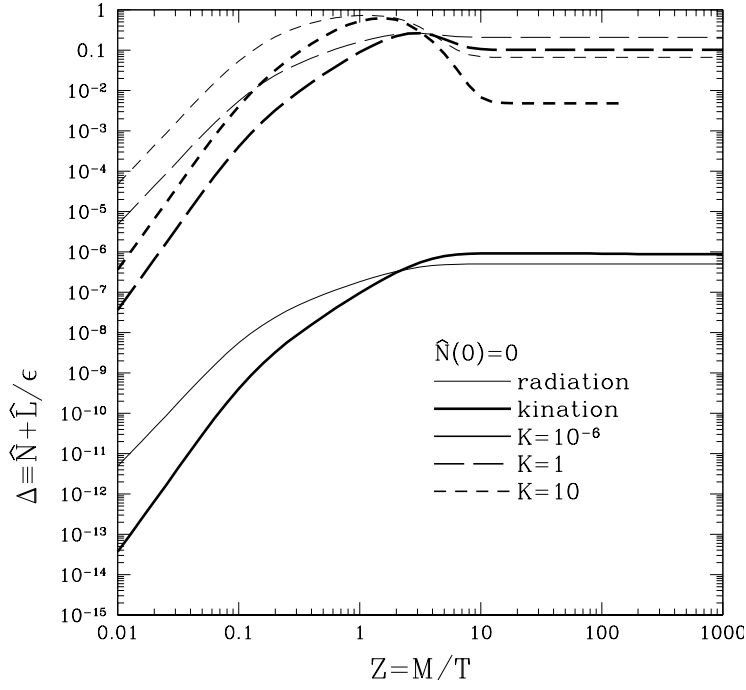


Figure 5: Evolution of $\Delta \simeq \hat{N} + \hat{L}/\epsilon$ as a function of z , with the boundary condition $\hat{N}(0) = 0$. Thin lines=radiation, thick lines=kination. Solid line, long dashes and short dashes for $K = 10^{-6}$, $K = 1$ and $K = 10$, respectively.

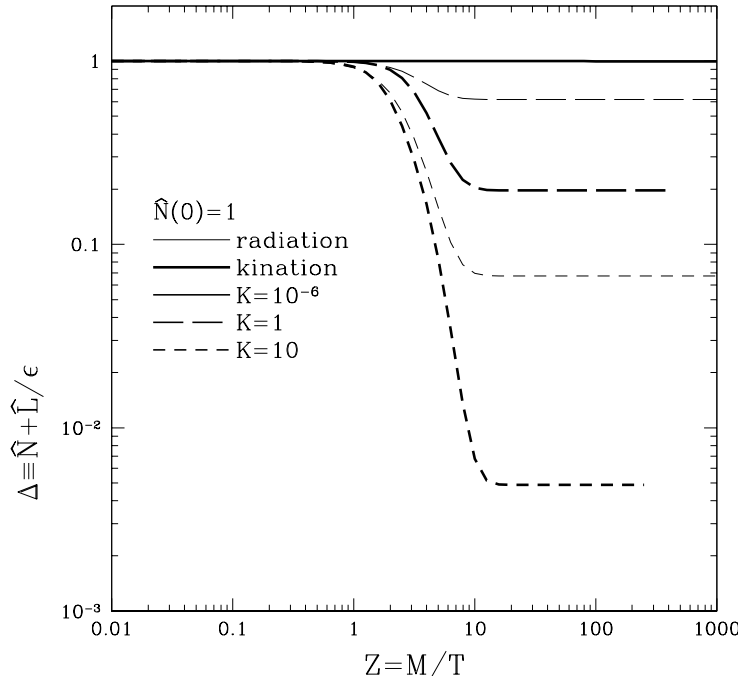


Figure 6: The same as in Fig. 5, for $\hat{N}(0) = 1$.

(iii) The efficiency in terms of K or (z_r, \tilde{m}) :

In Fig. 7 the efficiency \hat{L}/ϵ is plotted as a function of K . From this figure it is possible to summarize the various properties discussed above, comparing the cases of kination and radiation domination:

- curves for $\hat{N}(0) = 0$ and $\hat{N}(0) = 1$ differ at $K < 1$ (the latter saturating to 1) but coincide for $K > 1$;
- the effect of scattering is important for $K < 1$, implying in particular a large increase of the efficiency at very low K , but is negligible at $K > 1$;
- for $K > 1$ the efficiency for kination is about one order of magnitude smaller than for radiation [see Eqs. (25, 28)]; on the other hand the efficiencies are comparable in the two cases for $K \lesssim 1$ [see Eq. (23)].

We conclude this section by discussing the phenomenology of leptogenesis as a function of T_r , defined as the temperature for which the energy density of radiation and kination are the same. In Fig. 8 the efficiency is plotted as a function of the adimensional parameter $z_r \equiv \sqrt{\frac{g_*}{g_{*r}}} M/T_r$, for some representative values of the neutrino mass scale \tilde{m} . In this figure it is possible to see a smooth transition from radiation domination ($z_r \ll 1$) to kination domination ($z_r \gg 1$), and the following characteristic behaviors:

- super-weak wash-out regime with $z_r \gg 100$. Assuming $T_r \gtrsim 1$ MeV and taking into account the corresponding constraint $M \lesssim 10^5$ [see Eq. (10)] one gets the upper bound $z_r \lesssim 4.5 \times 10^8$. Assuming for instance $\tilde{m} = 0.05$ eV, this value of z_r corresponds in Fig. 8 to $K \lesssim \hat{L}/\epsilon \simeq 10^{-7}$. This situation has to be compared to the standard picture in which the energy density is dominated by radiation, corresponding, for the same curve, to the plateau at $z_r \ll 1$, for which $K \simeq 64$ and $\hat{L}/\epsilon \simeq 0.07$. So, if kination dominates the energy density of the Universe until nucleosynthesis, the corresponding efficiency for leptogenesis is suppressed by almost six orders of magnitude compared to the standard cosmology with radiation domination;
- increased efficiency with $1 \lesssim z_r \lesssim 100$. However, from the same figure it is possible to see that very different scenarios are possible by assuming $T_r \gg 1$ MeV. For instance, when $\tilde{m} \gtrsim 0.01$ eV the efficiency in the case of kination can be even larger compared to radiation for $1 \lesssim z_r \lesssim 100$. This can be explained by the fact that, for this range of \tilde{m} , the radiation dominated situation corresponds to a regime of strong washout, $K > 10$, while for kination it is possible to have $K \simeq 0.1$ – 1 , i.e. right in the interval that corresponds to a maximal efficiency. For instance, in Fig. 8 the maximum at $z_r \simeq 100$ for the curve with $\tilde{m}=0.05$ eV corresponds to $K \simeq 0.63$, which in Fig. 7 is the value of K where the efficiency is maximal for kination domination. On the other hand, this mechanism gets much more efficient and \hat{L}/ϵ is strongly suppressed for $z_r \gg 10^3$. Note that the possibility to increase the efficiency in the case of kination domination compared to radiation is easier for somewhat larger values of \tilde{m} . In fact, if one takes $\tilde{m} < 0.05$ eV, the value of K in the radiation dominated case becomes smaller. According to Fig. 7, when $K \simeq 1$ the efficiency for radiation is maximal, and this corresponds to $\tilde{m} \simeq 8 \times 10^{-4}$ eV. So, for $\tilde{m} < 8 \times 10^{-4}$ eV adding a period of kination always implies a lower efficiency.

5 Conclusions

We have discussed leptogenesis in the context of a cosmological model where the energy density of the early Universe is dominated by the kinetic term of a quintessence field during some epoch of its evolution. This assumption may lead to very different conclusions compared to the case of the standard cosmology, where the energy density of the Universe is dominated by radiation.

We have adopted as a free parameter the temperature T_r above which kination dominates over radiation, and shown that when T_r is set to its minimal value required by nucleosynthesis, $T_r \simeq 1$ MeV, gauge interactions can thermalize only at a temperature $T \lesssim 10^5$ GeV, so that the RHN mass $M \simeq T$ needs to be relatively light. This constraint is relaxed for higher values of T_r . Moreover, irrespective of T_r , we always find a sufficient window above the electroweak temperature $T \sim 100$ GeV for the sphaleron transition to thermalize and thus allow conversion of the lepton asymmetry to the observed baryon asymmetry.

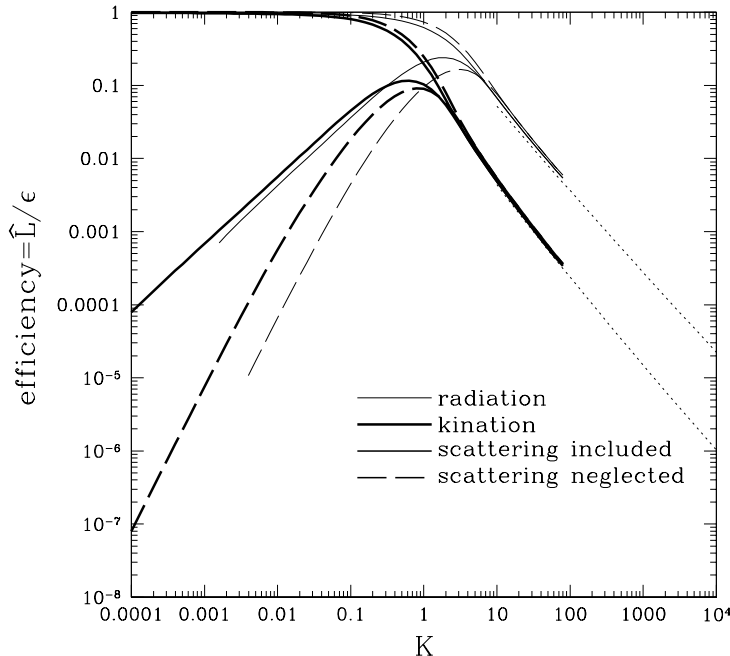


Figure 7: The efficiency $\eta = \hat{L}(z = \infty)/\epsilon$ as a function of K . Curves that saturate to 1 at $K \ll 1$ have a thermal initial distribution ($\hat{N}(0) = 1$) for RHNs, while those that vanish when $k \ll 1$ have $\hat{N}(0) = 0$. Thick lines: kination; thin lines: radiation; solid lines: scattering included; long dashes: scattering neglected. Dots: approximations given for $k \gg 1$ by Eqs. (26, 28, 29, 30).

When the RHN Yukawa coupling is fixed to get the observed neutrino mass scale $\simeq 0.05$ eV, in standard cosmology leptogenesis proceeds in the strong wash-out regime, $K \gg 1$. On the contrary, in kination leptogenesis any situation between the strong and the super-weak wash-out regime are equally viable by varying T_r . However, the effect of kination turns out to be either negligible or absent for models for which $K \gtrsim 10$ since the RHNs decay when radiation domination has already settled.

The weak wash-out regime is attained when $z_r \simeq M/T_r \gg 100$ for which the final efficiency for leptogenesis is approximately given by $\eta \simeq K \simeq (64/z_r)(\tilde{m}/0.05\text{eV})$, and can be several orders of magnitude smaller than that in the case of radiation domination for fixed \tilde{m} . In this case we have stressed the importance of s -channel scatterings driven by the top Yukawa coupling, which are the dominant process to create RHNs at high temperatures, and so enhance the leptogenesis efficiency by orders of magnitude in models where a vanishing initial RHN density is assumed. We remark that the condition $\eta \gtrsim 5 \times 10^{-8}$ for a successful leptogenesis $Y_{\hat{L}} = 4 \times 10^{-3}\epsilon\eta \approx 10^{-10}$ requires the upper bound on the RHN mass $M \lesssim 2.8 \times 10^5 \text{GeV}(T_r/\text{MeV})$, which is comparable to the thermal leptogenesis condition Eq. (10) for $T_r \sim 1$ MeV. On the other hand, when $1 \lesssim z_r \lesssim 100$ kination stops to dominate at a time which is not much later than when leptogenesis takes place: in this case, if $\tilde{m} \gtrsim 0.01$ eV, leptogenesis proceeds with $0.1 \lesssim K \lesssim 1$, in a regime where the efficiency is even better than the case of radiation domination.

We conclude that a wide range of possibilities opens up for leptogenesis if a period of kination-domination is assumed in the early Universe. The ensuing phenomenology can be parametrized as a function of only two parameters, $z_r \equiv \sqrt{\frac{g_*}{g_{*r}}}M/T_r$ and \tilde{m} .

Acknowledgment: We thank D. Chung for useful discussions.

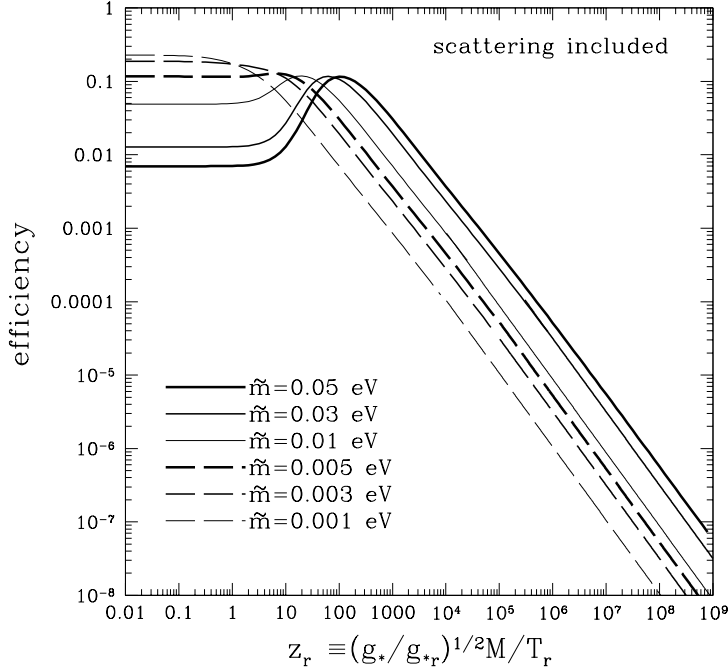


Figure 8: The efficiency as a function of $z_r \equiv \sqrt{g_*/g_{*r}} M/T_r$, for $N(0) = 0$ and for several values of \tilde{m} . A smooth transition between radiation domination (the plateau at $z_r \lesssim 1$) and kination-domination ($z_r \gtrsim 100$) is clearly visible.

References

- [1] R. R. Caldwell, R. Dave and P. J. Steinhardt, Phys. Rev. Lett. **80**, 1582 (1998) [arXiv:astro-ph/9708069].
- [2] P. J. Steinhardt, L. M. Wang and I. Zlatev, Phys. Rev. D **59**, 123504 (1999) [arXiv:astro-ph/9812313].
- [3] P. Salati, Phys. Lett. B **571**, 121 (2003) [arXiv:astro-ph/0207396]; F. Rosati, Phys. Lett. B **570**, 5 (2003) [arXiv:hep-ph/0302159]. S. Profumo and P. Ullio, JCAP **0311**, 006 (2003) [arXiv:hep-ph/0309220]; C. Pallis, JCAP **0510**, 015 (2005) [arXiv:hep-ph/0503080]; G. Barenboim and J. D. Lykken, JHEP **0612**, 005 (2006) [arXiv:hep-ph/0608265]; D. J. H. Chung, L. L. Everett, K. Kong and K. T. Matchev, arXiv:0706.2375 [hep-ph].
- [4] D. J. H. Chung, L. L. Everett and K. T. Matchev, arXiv:0704.3285 [hep-ph].
- [5] M. Fukugita and T. Yanagida, Phys. Lett. B **174**, 45 (1986); L. Covi, E. Roulet and F. Vissani, Phys. Lett. B **384**, 169 (1996).
- [6] P. Arnold, D. Son and L. G. Yaffe, Phys. Rev. D **55**, 6264 (1997); D. Bodeker, Phys. Lett. B **426**, 351 (1998); G. D. Moore and C. Hu and B. Muller, Phys. Rev. D **58**, 045001 (1998).
- [7] M. Plümacher, Nucl. Phys. B **530**, 207 (1998) [arXiv:hep-ph/9704231].
- [8] G. F. Giudice, A. Notari, M. Raidal, A. Riotto and A. Strumia, Nucl. Phys. B **685**, 89 (2004) [arXiv:hep-ph/0310123].
- [9] W. Buchmuller, P. Di Bari and M. Plumacher, Annals Phys. **315**, 305 (2005) [arXiv:hep-ph/0401240].